Overexpression of small ubiquitin-like modifier 2 ameliorates high glucose-induced reductions in cardiomyocyte proliferation via the transforming growth factor-β/Smad pathway

CHEN ZHAO and QILE SHEN

Department of Geriatric, Shanghai Tongren Hospital,
Shanghai Jiaotong University School of Medicine, Shanghai 200336, P.R. China

Received August 1, 2017; Accepted December 12, 2017

DOI: 10.3892/mmr.2018.9522

Abstract. Hyperglycemia may induce diabetic cardiomyopathy (DC). In the current study, the mechanism underlying the alleviation of high glucose (HG)-induced impairments in the proliferation of H9c2 embryo cardiomyocyte proliferation by small ubiquitin-like modifier 2 (SUMO2) overexpression was investigated. H9c2 cell morphology was identified as classical long shuttle type by optical microscopy. The viability of HG-injured H9c2 cells was evaluated by a Cell Counting Kit-8 assay and the results indicated that viability was inhibited in a dose-dependent (5.6, 10, 20 and 30 mmol/l) and time-dependent (6, 12 and 24 h) manner. H9c2 cells treated with 20 mmol/l HG for 24 h were selected for subsequent experiments due to the extent of injury caused at a low density. Flow cytometry was conducted to confirm cell cycle arrest between G_1/S phases and apoptosis promotion in HG-injured H9c2 cells, and the subsequent alleviating effect of SUMO2 overexpression on these HG-induced effects. Reverse transcription-quantitative polymerase chain reaction (RT-qPCR) and western blot analysis were performed to detect mRNA and protein expression levels of cell cycle-and apoptosis-associated factors. The results indicated that the expression ofthe cell cycle-associated factors CyclinA2 and C-Myc was upregulated, and cyclin-dependent kinase inhibitor 1a was downregulated. The expression of the apoptosis-associated factor Bcl-2 was upregulated, while Bcl-2-associated X and caspase-3 expression was downregulated, by SUMO2 overexpression. Furthermore, the effect of SUMO2 overexpression on the transforming growth factor (TGF)-β/Smad pathway was also determined using RT-qPCR and western blot analysis. The results indicated the mRNA and protein levels of TGF-β1 and Smad3 in HG-injured H9c2 cells were significantly decreased following SUMO2 overexpression. Thus, the results demonstrated that overexpression of SUMO2 may alleviate H9c2 cardiomyocyte cell cycle arrest and apoptosis promotion induced by HG via regulation of cell cycle- and apoptosis-associated factors, as well as inhibition of the TGF-β/Smad pathway. These results may therefore provide a novel strategy for the protection of cardiomyocytes and may aid the diagnosis and prognosis of patients with DC.

Correspondence to: Dr Qile Shen, Department of Geriatric, Shanghai Tongren Hospital, Shanghai Jiaotong University School of Medicine, 1111 Xianxia Road, Shanghai 200336, P.R. China
E-mail: sql1801@shtrhospital.com

Key words: small ubiquitin-like modifier 2, high glucose, cardiomyocytes, cell cycle, transforming growth factor-β/Smad pathway, apoptosis

Introduction

Cardiovascular disease (CVD) accounts for 16.7 million deaths every year, and is one of the leading causes of deaths worldwide (1,2). Hyperglycemia is an important factor in the induction of myocardial dysfunction and heart failure in patients with diabetes (3). Clinical evidence has demonstrated that elevated blood glucose levels may result in the development of diabetic cardiomyopathy (DC) (4). DC is a major complication that increases the incidence and mortality of patients with diabetes, and is a unique myocardial disease occurring independently of hypertension and coronary atherosclerosis (5). DC induces ischemic myocardial injury and cardiac hypertrophy, which contributes to the cardiac failure of patients with diabetes (6), and it is a complication of hypertension and coronary artery disease (7). In addition, as an independent cause of heart failure, it may be possible to reduce the incidence and mortality of heart failure by preventing cardiac hypertrophy. There are currently no effective treatments for DC; therefore, investigation into the molecular mechanisms of DC and cardiac hypertrophy may identify novel therapeutic strategies for heart failure in patients with diabetes.

The majority of cardiomyocytes stop differentiating and proliferating soon after birth. However, certain cardiomyocytes re-enter into the cell cycle when stimulated by stress (8), thereby inducing the excessive increase of nucleic acids and proteins. Cell sizes enlarge without increasing cell numbers, eventually inducing cardiac hypertrophy and heart failure (2,9). Apoptosis is a major mechanism of cell death that consists of a series of tightly regulated cascades of molecular processes (10). Sustained hyperglycemia may induce the

apoptosis of cardiomyocytes in patients with diabetes (11,12). It has also been demonstrated that cardiomyocyte apoptosis serves a prominent role in the pathogenesis of DC (13).

Small ubiquitin-like modifiers (SUMOs) are highly conserved ubiquitin-like proteins and 18% of their sequence is homologous with ubiquitin. There are four distinct SUMO isoforms (SUMO1, SUMO2, SUMO3 and SUMO4) in mammals (14). SUMOs primarily function in protein post-translational modification, modify the stability and interactions of proteins and regulate signal transduction (15,16). SUMO1 primarily modifies physiological proteins, while SUMO2 and SUMO3 have similar amino acid sequences and primarily modify stress proteins associated with oxidative stress, heat shock and osmotic pressure (17). The function of SUMO4 remains unclear and its expression is detected in a limited number of tissues, including the kidney, spleen and lymph node (18,19). SUMOylation serves important roles in physiological processes and the development of various diseases, including inflammation, cancer and nervous lesions (20-23). It has also been demonstrated that SUMOylation serves important roles in the regulation of apoptosis in DC (24,25).

Transforming growth factor (TGF)-β is associated with organ fibrosis and hypertrophy (12-14). The TGF-β/Smad pathway regulates cell differentiation, proliferation, migration and apoptosis and maybe adjusted by post-translational modifications such as phosphorylation, acetylation and ubiquitylation. It has been demonstrated that the TGF-β/Smad pathway may be activated by high glucose (HG) via regulation of the expression levels of Smad2 and Smad3, and the pathway contributes to the fibrotic interstitium in DC (13,26,27). Previous studies have also indicated that SUMO is involved in the regulation of the TGF-β/Smad pathway (28,29). However, the role served by the modifying effect of SUMOylation on the TGF-β/Smad pathway in DC remains unclear.

In the present study, the effect of SUMO2 overexpression on HG-injured cardiomyocyte cell cycle and apoptosis was investigated. The effect of SUMO2 overexpression on the TGF-β/Smad pathway was subsequently evaluated. The results may provide novel insights into SUMO2 as a potential biomarker for the treatment of DC.

Materials and methods

Cell culture. H9c2 rat embryo cardiomyocytes purchased from the American Type Culture Collection (Manassas, VA, USA) were cultured in Dulbecco's modified Eagle's medium (DMEM; Gibco; Thermo Fisher Scientific, Inc., Waltham, MA, USA) supplemented with 10% fetal bovine serum (Gibco; Thermo Fisher Scientific, Inc.) and 100 U/ml penicillin/streptomycin (Invitrogen; Thermo Fisher Scientific, Inc.) at 37˚C with 5% CO_2. Cells at logarithmic phase were used in the current study. H9c2 cell morphology was identified under an Olympus DSX100 optical microscope (Olympus Corporation, Tokyo, Japan) at 48 h following treatment (magnification, x100 or 200).

Cell viability assay. H9c2 cells were randomly divided into the following five groups: HG groups treated with HG (Sigma-Aldrich; Merck KGaA, Darmstadt, Germany) under normal glucose concentration (5.6 mmol/l) and three different HG concentrations (10, 20 and 30 mmol/l); and a control group without any treatment (n=5 each group). Cell viabilities were measured using a Cell Counting Kit (CCK)-8 assay (Beyotime Institute of Biotechnology, Haimen, China) following HG administration for different durations (6, 12 and 24 h). Following treatment, cells were seeded in 96-well plates at an initial density of $5x10^3$ cells/well and incubated for the indicated durations at 37˚C. A total of 20 μl CCK-8 reagent was subsequently added into each well of the plate and plates were incubated at 37˚C for 1 h. The optical density values were read at 450 nm by a microplate reader (Bio-Tek Instruments, Inc., Winooski, VT, USA). Data were expressed as the percentage of viable cells as follows: Relative viability (%) = $[A_{450}(\text{treated})-A_{450}(\text{blank})]/[A_{450}(\text{control})-A_{450}(\text{blank})]$ x100.

Cell transfection. Cell transfection was performed following construction of a SUMO2 overexpression plasmid with the pGEM-T/pFLAGvector (Promega Corporation, Madison, WI, USA) and Lipofectamine 2000 (Invitrogen; Thermo Fisher Scientific, Inc.) was used as the transfection reagent. The empty vector was transfected respectively at the same time as a transfection negative control group. Cells were inoculated in DMEM culture media without antibiotics. SUMO2 plasmid (4 μg) and Lipofectamine 2000 (10 μl) were added into DMEM culture media without serum (or opti-MEM media) when cell density reached 90-95%, and mixed gently with the dilution of 1:2 (DNA: Lipofectamine 2000). The culture media was changed into DMEM with 10% fetal bovine serum following culture for 6 h at 37˚C with 5% CO_2. The cell transfection rates were detected by reverse transcription-quantitative polymerase chain reaction (RT-qPCR) and western blot analysis following culture for 48 h.

Cell group division. Cells were divided into five experimental groups to perform the subsequent experiments: SUMO+HG group, consisting of H9c2 cells treated with 20 mmol/l HG for 24 h following transfection with SUMO2 overexpression plasmid for 12 h; Vect+HG group, consisting of H9c2 cells treated with 20 mmol/l HG for 24 h following transfection with empty plasmid vector for 12 h; Vect group, consisting of H9c2 cells only transfected with empty plasmid vector for 12 h; HG group, consisting of H9c2 cells treated with 20 mmol/l HG for 24 h only; and control group, consisting of H9c2 cells without any treatment.

RT-qPCR. mRNA expression levels were measured using RT-qPCR. Total RNA was extracted from cells in each experimental group using an RNeasy kit (Qiagen, Inc., Valencia, CA, USA) and cDNA was reverse transcribed with 1 μg RNA at 42˚C, for 60 min, using a QuantiTect Reverse Transcription kit (Qiagen, Inc.), according to the manufacturer's protocol. The qPCR amplification was performed for 15 sec at 95˚C, followed by 40 cycles of denaturation at 95˚C for 15 sec and annealing/extension at 60˚C for 15 sec in an ABI 7300 Thermocycler (Applied Biosystems; Thermo Fisher Scientific, Inc.) using a Fast SYBR Green Master Mix (Applied Biosystems; Thermo Fisher Scientific, Inc.). The quantification was identified by $2^{-\Delta\Delta Cq}$ (30). Expression levels were normalized to that of GAPDH; the oligonucleotide primer sequences use dare presented in Table I.

Table I. Primers used in reverse transcription-quantitative polymerase chain reaction analysis.

Gene	Orientation	Sequence
SUMO2	Forward	GACGAGAAACCCAAGGA
	Reverse	CTGCCGTTCACAATAGG
CyclinA2	Forward	TGATGAAACTATGACCATGATGTCC
	Reverse	TTCACAGAACGCAGACCACC
CDKN1a	Forward	TTGTCGCTGTCTTGCACTCT
	Reverse	GGCACTTCAGGGCTTTCTC
C-Myc	Forward	GGTGGAAAACCCGACAGTCA
	Reverse	GCAACATAGGACGGAGAGCA
Bcl-2	Forward	CCCCTGGCATCTTCTCCTTCC
	Reverse	GGGTGACATCTCCCTGTGACG
Bax	Forward	GGATGCGTCCACCAAGAA
	Reverse	ACGGAGGAAGTCCAGTGT
Caspase-3	Forward	GCCTCTGCCCGGTTAAGAAA
	Reverse	CATCTGTACCAGACCGAGCG
TGF-β1	Forward	CGCCTGCAGAGATTCAAGTC
	Reverse	GCCCTGTATTCCGTCTCCTT
Smad3	Forward	GTCATCTACTGCCGCTTGTG
	Reverse	GGGGATGGAATGGCTGTAGT
GAPDH	Forward	GGTCATGAGTCCTTCCACGATA
	Reverse	ATGCTGGCGCTGAGTACGTC

SUMO2, small ubiquitin-like modifier 2; CDKN1a, cyclin-dependent kinase inhibitor 1a; Bax, Bcl-2-associated X; TGF-β1, transforming growth factor-β1.

Western blot analysis. Cells were lysed by protein lysis reagent P0013 from Beyotime Institute of Biotechnology (Haimen, China), followed by centrifugation at 10,000 x g for 5 min at 4˚C, and the supernatants containing proteins were collected. Protein concentration was determined by a BCA assay (Beyotime Institute of Biotechnology). Proteins (10 μg) were subsequently subjected to each lane of 12% SDS-PAGE and electro blotted onto polyvinylidene difluoride (PVDF) membranes (GE Healthcare, Chicago, IL, USA). Following blocking with 5% nonfat dry milk in PBS for 1 h at 37˚C, the blotting membranes were probed overnight at 4˚C with primary antibodies including rabbit anti-SUMO2 (1:2,000; ab209822), CyclinA2 (1:2,000; ab137769), CDKN1a (1:1,000; ab109199), C-Myc (1:1,000; ab39688), anti-B-cell lymphoma-2 (Bcl-2; 1:1,000; ab196495), anti-Bcl-2-associated X (Bax; 1:1,000; ab53154), anti-active-caspase-3 (1:200; ab2302), Smad3 (1:1,000; ab84177), TGF-β1 (1:1,000; ab92486) and anti-GAPDH (1:2,500; ab9485) (all from Abcam, Cambridge, UK). Then the membranes were subsequently probed with the appropriate horseradish peroxidase (HRP)-conjugated secondary antibodies: Goat anti-rabbit IgG H&L HRP (1:5,000; ab6721; Abcam). The PVDF membrane was exposed to X-ray film and immunoreactive bands were detected by reaction with enhanced chemiluminescence (ECL) detection system reagent, GE ECL Start (GE Healthcare). The membrane was probed with a monoclonal antibody for GAPDH as the loading control. Band densities were quantified by densitometry with Bio-Rad ChemiDoc XRS$^+$ (Bio-Rad Laboratories, Inc., Hercules, CA, USA).

Cell cycle analysis. Cell cycle progression was evaluated by propidium iodide (PI) staining. Cells ($5.0x10^5$/ml) from each group were trypsinized, washed twice using PBS and fixed overnight at 4˚C in ice-cold 70% ethanol. Following two washes with PBS, cells were incubated in 50 μg/ml PI (Invitrogen; Thermo Fisher Scientific, Inc.) and 100 μg/ml RNase (Thermo Fisher Scientific, Inc.) for 30 min at room temperature. Thereafter, analysis was immediately performed using FACSCalibur flow cytometer and BD CellQuest™ Pro Software (BD Biosciences, Franklin Lakes, NJ, USA). The proportion of cells in G_0/G_1, S and G_2/M phases was subsequently detected.

Apoptosis detection. The apoptosis status of the cells in each group was determined by an Annexin V-fluorescein isothiocyanate (FITC) Apoptosis kit (BioVision, Inc., Milpitas, CA, USA), according to the manufacturer's protocols. Briefly, floating and trypsinized adherent cells ($5x10^5$) from each group were collected and re suspended in 500 μl PBS containing 5 μl Annexin V-FITC and 5 μl PI, and incubated for 5 min in the dark at room temperature. Analysis was subsequently performed using a flow cytometer (BD Biosciences). Cell Quest Pro software (BD Biosciences) was used to analyze the apoptosis rate.

Statistical analysis. Data are presented as the mean ± standard deviation of five independent experiments. Statistical analysis was performed using SPSS 18.0 (SPSS, Inc., Chicago, IL, USA) and data were subjected to one-way analysis of variance followed by a Dunnett's post-hoc test. $P<0.05$ was considered to indicate a statistically significant difference.

Results

Cell morphology. H9c2 cells are rat embryo myocardial cells. Cell morphology was identified under an optical microscope. Cells grew well and were adherent to the bottom of culture flasks as a monolayer at 48 h following treatment. The majority of cells appeared to exhibit long-shuttle morphology and certain cells had a triangular or irregular morphology (Fig. 1A).

Inhibitory effect of HG on H9c2 cell viability. Cell viability was evaluated by a CCK-8 assay following HG treatment of H9c2 cells at different concentrations (0, 5.6, 10, 20 and 30 mmol/l) for different durations (6, 12 and 24 h) to indicate the damage induced by HG on H9c2 cells. The results indicated that H9c2 cell viability decreased in a dose-dependent and time-dependent manner. The viability was significantly decreased by 42% compared with the control group when treated with 20 mmol/l HG for 24 h ($P<0.05$) and was similar to cells treated with 30 mmol/l HG for 24 h (Fig. 1B). Therefore, H9c2 cells treated with 20 mmol/l HG for 24 h were selected for subsequent experiments due to the extent of cytotoxicity at a low density (HG group).

Transfection rates of overexpressed SUMO2 in H9c2 cells. The transfection efficiency in each group was determined by

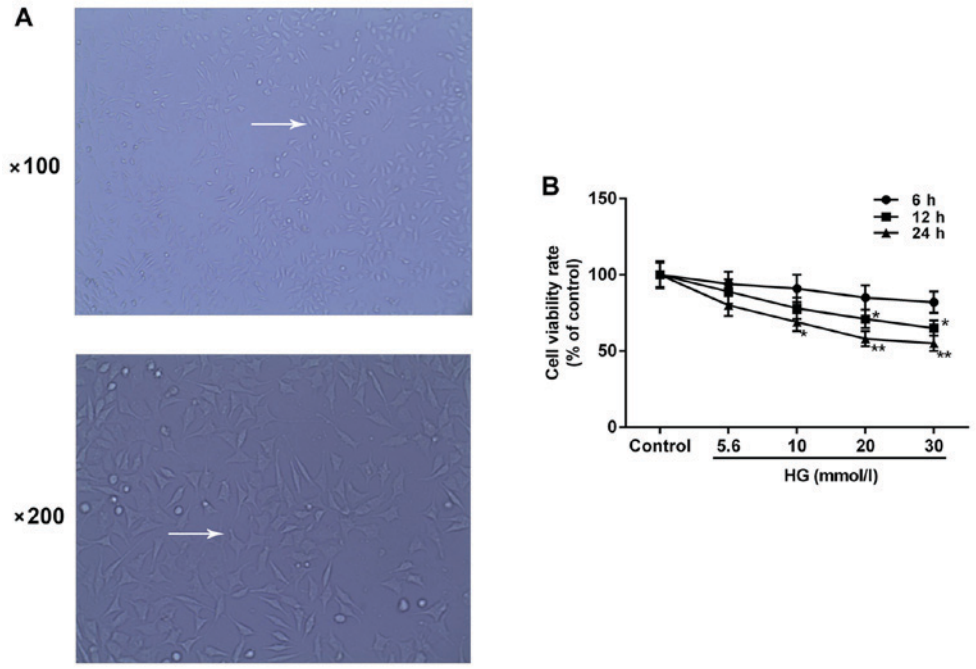

Figure 1. Cell morphology and the effect of HG on H9c2 cell viability. (A) H9c2 cell morphology was observed by optical microscopy at 48 h following HG treatment. Magnification, x100 and x200. H9c2 cells were pointed out by arrows too. (B) Inhibitory effect of HG on H9c2 cell viability was detected by a cell counting kit-8 assay following treatment of H9c2 cells with HG (0, 5.6, 10, 20 and 30 mmol/l) for different durations (6, 12 and 24 h). Data are presented as the mean ± standard deviation, n=5 per group. *P<0.05 and **P<0.01 vs. control group at the same time-point. HG, high glucose.

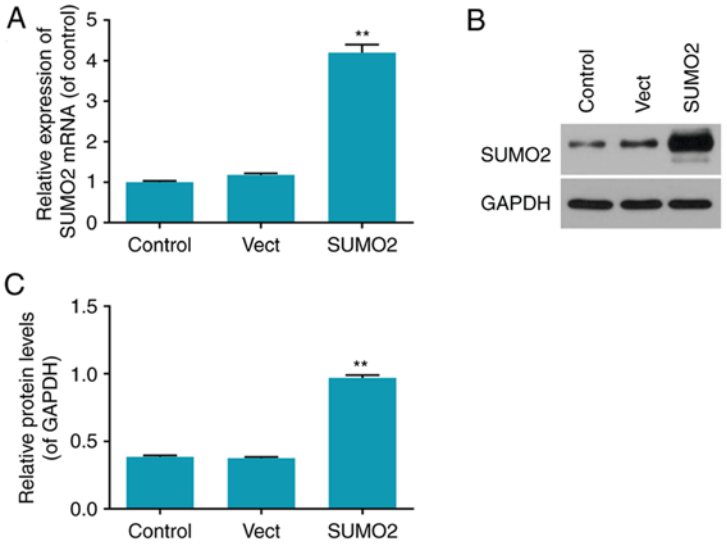

Figure 2. H9c2 cell transfection rates of overexpressed SUMO2. (A) Efficiency of transfection of H9c2 cells with SUMO2 overexpression plasmid was determined by reverse transcription-quantitative polymerase chain reaction. (B) Efficiency of transfection of H9c2 cells with SUMO2 overexpression plasmid was also determined by western blot analysis. SUMO2 and SUMO3 have similar sequences, therefore the majority of antibodies recognize both of them at the same time and this accounts for the multiple bands presented here. (C) Quantification of western blot analysis was performed with densitometry software. Data are presented as the mean ± standard deviation, n=5 per group. **P<0.01 vs. control group. SUMO, small ubiquitin-like modifier; Vect, empty vector.

RT-qPCR and western blot analysis (Fig. 2). The mRNA and protein levels of SUMO2 were significantly increased in the SUMO2 group compared with the control (P<0.01; Fig. 2). The mRNA and protein levels of SUMO2 in the Vect group transfected with empty vector were not significantly different from the control group (Fig. 2).

Effect of SUMO2 overexpression on HG-induced H9c2 cell cycle arrest. The viability of HG-treated cells was decreased, therefore, the subsequent effect of SUMO2 overexpression on H9c2 cell cycle progression was investigated by flow cytometry. Treatment of H9c2 cells with HG blocked the cell cycle transition from G_1 to S phase (Fig. 3A and B). The percentage of cells in G_0/G_1 phases significantly increased from 41.97 to 59.58% (P<0.05), while the S phase fraction decreased from 38.45 to 29.60% (P<0.05), in the HG group compared with the control group (Fig. 3A and B). Following SUMO2 overexpression, the cell cycle transition from G1 to S phase

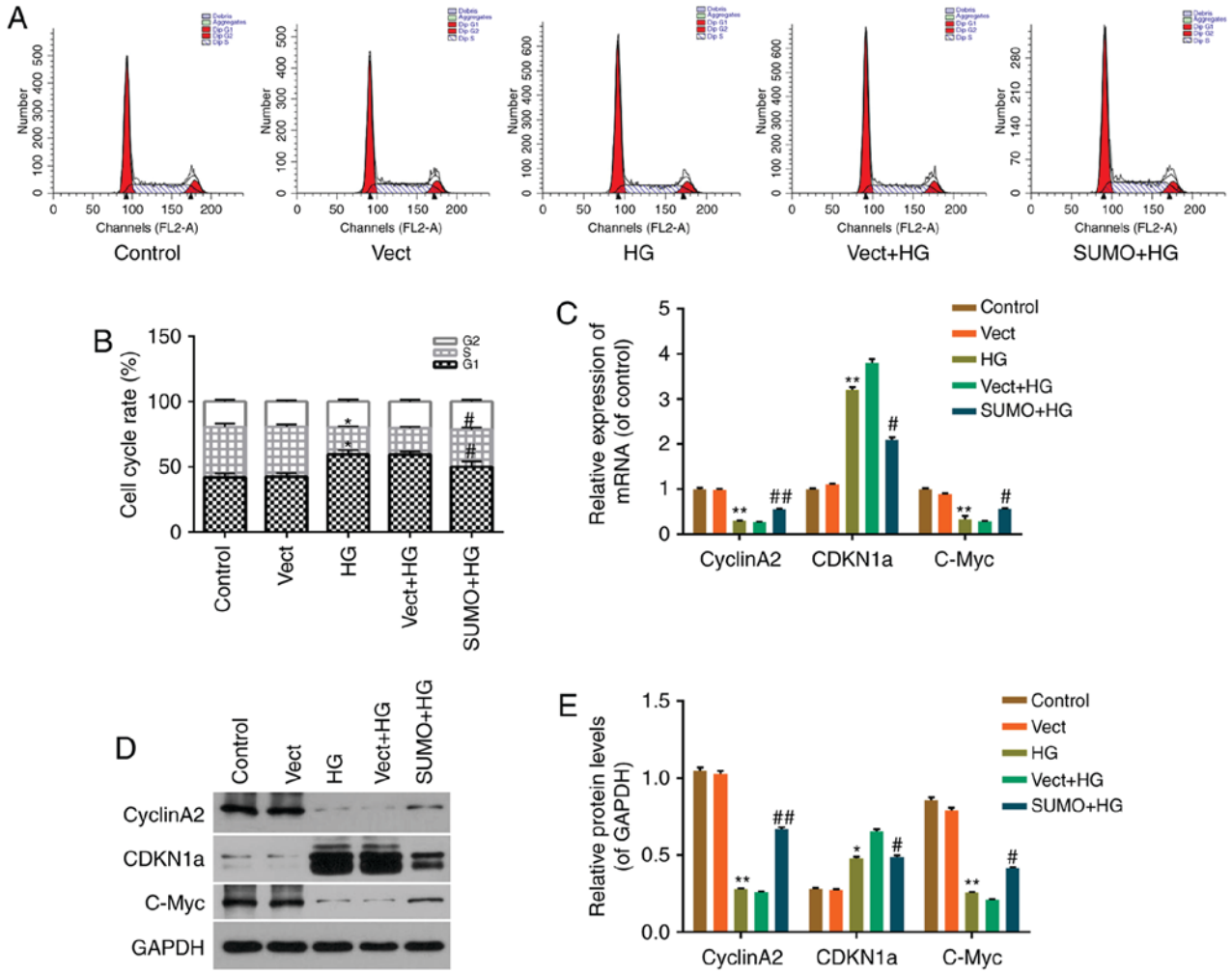

Figure 3. Effect of SUMO2 overexpression on the cell cycle and cell cycle-associated factors in HG-injured H9c2 cells. (A) Flow cytometry was applied to detect the cell cycle progression in each group. (B) Quantification of flow cytometry analysis. (C) Reverse transcription-quantitative polymerase chain reaction was performed to detect mRNA levels of the cell cycle-associated factors CyclinA2, CDKN1a and C-Myc in each group. (D) Western blot analysis was performed to detect protein levels of CyclinA2, CDKN1a and C-Myc in each group. Note that the specificity of the CDKN1a antibody may not have been sufficient to recognize one specific band. (E) Quantification of western blot analysis was performed with densitometry software. Data are presented as the mean ± standard deviation, n=5 per group. *P<0.05 and **P<0.01 vs. control group; $^{\#}$P<0.05 and $^{\#\#}$P<0.01 vs. Vect+HG group. SUMO2, small ubiquitin-like modifier 2; HG, high glucose; CDKN1a, cyclin-dependent kinase inhibitor 1a; Vect, empty vector.

recovered significantly, the percentage of cells in G_0/G_1 phases significantly decreased from 59.44 to 50.06% (P<0.05), while the S phase fraction significantly increased from 20.06 to 28.44% (P<0.05) in the SUMO + HG group compared with the Vect+HG group (Fig. 3A and B).

Effect of SUMO2 on cell cycle-associated factors in H9c2 cells treated with HG. To investigate the mechanism by which SUMO2 overexpression protects H9c2 cells from HG-induced cell viability inhibition and cell cycle arrest, RT-qPCR and western blot analysis were performed. mRNA and protein levels of cell cycle-associated factors, including CyclinA2, CDKN1a and C-Myc, were detected in each group. The results indicated that the mRNA and protein levels of CDKN1a were significantly increased in the HG group compared with the control group (P<0.01 and P<0.05, respectively) and significantly decreased in the SUMO+HG group compared with the Vect+HG group (both P<0.05; Fig. 3C-E). By contrast, the mRNA and protein levels of CyclinA2 and C-Myc were significantly decreased in the HG group compared with the control group (all P<0.01) and significantly increased in the SUMO+HG group compared with the Vect+HG group (P<0.05; Fig. 3C-E).

Inhibitory effect of SUMO2 overexpression on HG-induced H9c2 cell apoptosis. The inhibition of apoptosis by SUMO2 following HG treatment was investigated by performing an Annexin V/PI double-stain assay to detect the apoptosis status in each group. The apoptosis rate of the HG group was significantly increased compared with the control group (P<0.01) and the apoptosis rate of the SUMO+HG group was significantly decreased by ~42% of that of the Vect+HG group (P<0.01; Fig. 4A and B). Thus, the results indicated that SUMO2 overexpression may inhibit the promotion of H9c2 cell apoptosis by HG.

Effect of SUMO2 overexpression on apoptosis-associated factors in H9c2 cells treated with HG. To investigate the mechanism by which SUMO2 overexpression protects H9c2 cells from HG-induced inhibition of cell viability

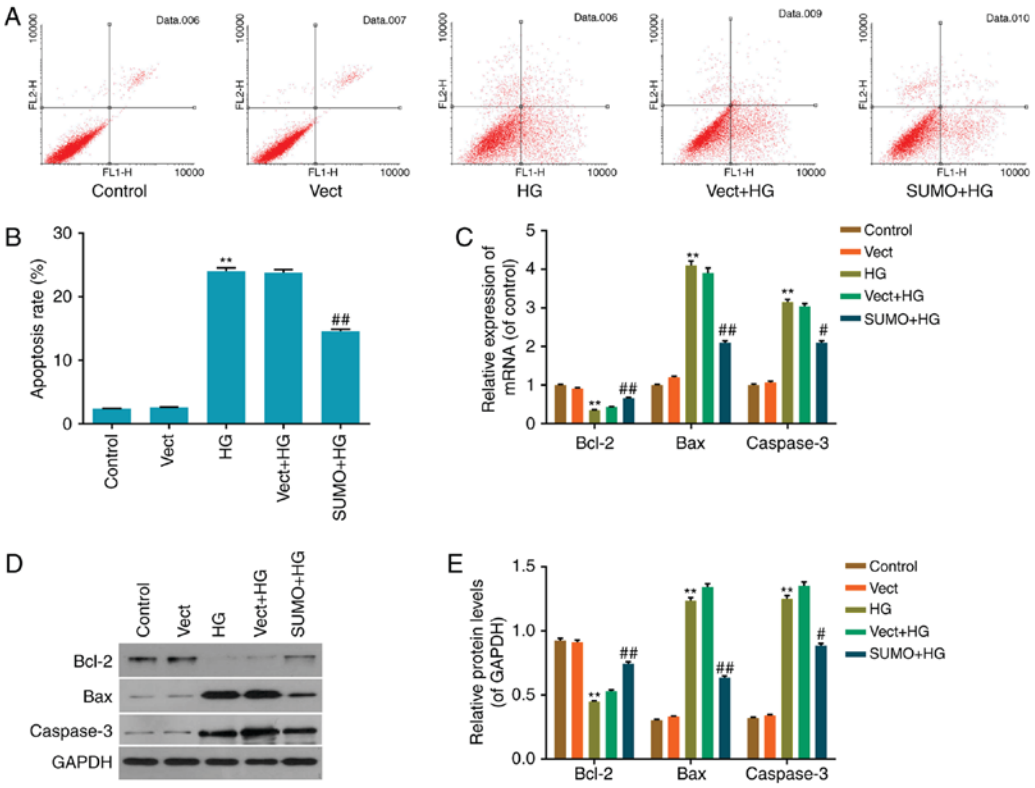

Figure 4. Effect of SUMO2 overexpression on apoptosis and apoptosis-associated factors in HG-injured H9c2 cells. (A) Annexin V/propidium iodide double-stain assay and flow cytometry were applied to detect the apoptosis status cells in each group. Upper right + lower right quadrants were considered as apoptotic cells. (B) Quantification of the apoptosis rate in each group. (C) Reverse transcription-quantitative polymerase chain reaction was performed to detect mRNA levels of the apoptosis-associated factors Bax, Bcl-2 and Caspase-3 in each group. (D) Western blot analysis was performed to detect the protein levels of Bax, Bcl-2 and Caspase-3 in each group. (E) Quantification of western blot analysis was performed with densitometry software. Data are presented as the mean ± standard deviation, n=5 per group. **P<0.01 vs. control group; $^{\#}$P<0.05 and $^{\#\#}$P<0.01 vs. Vect+HG group. SUMO2, small ubiquitin-like modifier 2; HG, high glucose; Bax, Bcl-2-associated X; Vect, empty vector.

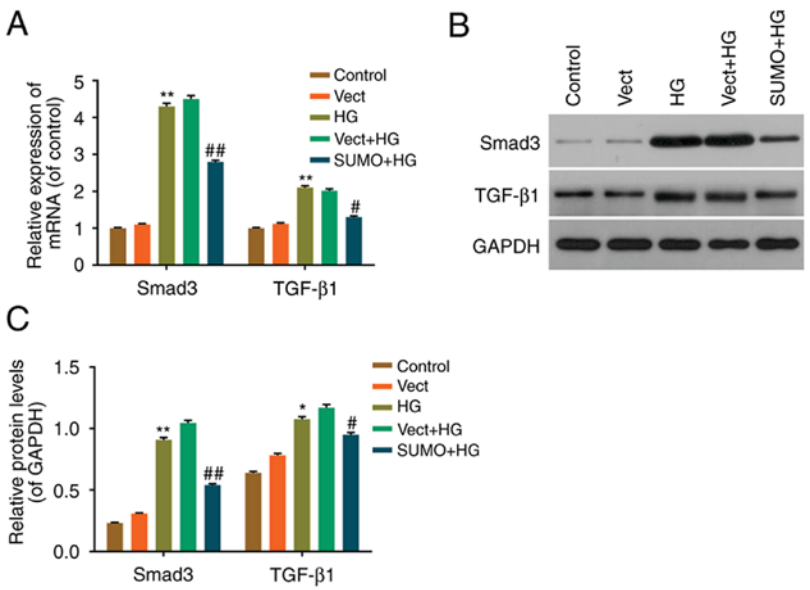

Figure 5. Effect of SUMO2 overexpression on the TGF-β/Smad pathway in HG-injured H9c2 cells. (A) Reverse transcription-quantitative polymerase chain reaction was performed to detect the mRNA levels of TGF-β1 and Smad3 in each group. (B) Western blot analysis was performed to detect the protein levels of TGF-β1 and Smad3 in each group. (C) Quantification of western blot analysis was performed with densitometry software. Data are presented as the mean ± standard deviation, n=5 per group. *P<0.05 and **P<0.01 vs. control group; $^{\#}$P<0.05 and $^{\#\#}$P<0.01 vs. Vect+HG group. SUMO2, small ubiquitin-like modifier 2; TGF-β, transforming growth factor-β; HG, high glucose; Vect, empty vector.

inhibition and apoptosis promotion, RT-qPCR and western blot analysis were performed to detect mRNA and protein levels of apoptosis-associated factors, including Bax, Bcl-2 and Caspase-3, in each group. The results indicated that the

mRNA and protein levels of the apoptosis activating factors Bax and Caspase-3 were significantly increased in the HG group compared with the control group (P<0.01) and significantly decreased in the SUMO+HG group compared with the Vect+HG group (P<0.05; Fig. 4C-E). By contrast, the mRNA and protein levels of the apoptosis inhibitor Bcl-2 were significantly decreased in the HG group compared with the control group (P<0.01) and significantly increased in the SUMO+HG group compared with the Vect+HG group (P<0.01; Fig. 4C-E).

Effect of SUMO2 overexpression on the TGF-β/Smad pathway in H9c2 cells treated with HG. The effect of SUMO2 overexpression on downstream effectors in the TGF-β/Smad pathway was also investigated. RT-qPCR and western blot analysis were performed to assess the mRNA and protein levels of TGF-β1 and Smad3. The expression of TGF-β1 and Smad3 mRNA and protein was significantly increased in the HG group compared with the control group (P<0.05) and significantly decreased in the SUMO+HG group compared with the Vect+HG group (P<0.05) (Fig. 5). These results therefore indicated that SUMO2 overexpression may inhibit cell apoptosis by regulating the TGF-β/Smad pathway in H9c2 cells treated with HG.

Discussion

Hyperglycemia is an inducing factor of DC, which increases the mortality of patients with diabetes and is characterized by cardiac hypertrophy (31,32). Investigation of the molecular mechanisms of DC and cardiac hypertrophy may uncover novel therapeutic strategies for heart failure in patients with diabetes. It may be hypothesized that SUMOs may aid in treating DC, as they have an important modification function in physiological process and disease development (17,33,34).

The current study investigated how overexpression of SUMO2 affected HG-induced cardiomyocyte injury, with a focus on the cell cycle and apoptosis. H9c2 rat embryo cardiomyocytes with a classical long shuttle type morphology, identified by optical microscopy, were employed in the current study. The viability of HG-injured H9c2 cells was evaluated by a CCK-8 assay and the results indicated that the viability was decreased in a dose-dependent (0, 5.6, 10, 20 and 30 mmol/l) and time-dependent (6, 12 and 24 h) manner. The degree of inhibition on cell viability with 30 mmol/l HG was more than that of 20 mmol/l, however, the increase was not significant. Therefore, H9c2 cells treated with 20 mmol/l HG for 24 h were selected for subsequent experiments.

The cell cycle is the process by which a cell divides into two daughter cells and it consists of interphase (G_1, S and G_2 phases) and mitotic (M) phase (35). Cell cycle regulatory factors, which include cyclin, CDKs and CDK inhibitors, serve critical roles in the regulation of the cell cycle (36-38). Different combinations of cyclins and CDKs control cell cycle progression. Cardiac hypertrophy occurs when cardiomyocytes grow without division, during which cell cycle regulatory factors may serve prominent roles (39,40). The results of the current study indicated that the cell cycle was blocked between G_1/S phases when H9c2 cells were treated with 20 mmol/l HG for 24 h and the blocking effect was attenuated by SUMO2 overexpression. RT-qPCR and western blot analysis were performed to determine the underlying molecular mechanisms of this effect of SUMO2 overexpression. The results demonstrated that the expression of the cell cycle activating factors CyclinA2 and C-Myc were downregulated by HG and upregulated by SUMO2 overexpression in HG-injured H9c2 cells. By contrast, the expression of CDKN1a, also termed p21, was upregulated by HG and downregulated by SUMO2 overexpression in HG-injured H9c2 cells. The combination of CyclinA2 with CDKs serves critical roles in the transition of the cell cycle from G_1/S phase to G_2/M phase, which promotes cell mitosis (41,42), and C-Myc encodes a phosphoprotein that facilitates cell proliferation and differentiation (43,44). CDKN1a is a critical negative regulator in the cell cycle that inhibits the activation of Cyclin and CDK complexes (45,46). Hence, SUMO2 overexpression may attenuate cell cycle arrest induced by HG in H9c2 cells via regulation of cell cycle-associated factors, by inhibiting the cyclin transition-promoting function of CyclinA2, the cycle promoting function of C-Myc and inhibiting the function of CDKN1a.

In addition to the cell cycle, there is evidence indicating that apoptosis constitutes the prevailing form of myocyte death (47-49). Cardiomyocyte apoptosis was reported to be the pathophysiological basis of the development of DC and to account for the high incidence of heart failure (11,13).Therefore, it is critical to further investigate the molecular mechanism of cardiomyocyte apoptosis. Annexin V/PI double-stain assay and flow cytometry were performed in the current study to determine whether SUMO2 overexpression affects cell apoptosis stimulated by HG, and the results demonstrated that SUMO2 overexpression decreased the rate of apoptosis induced by HG in H9c2 cells. The results of RT-qPCR and western blotting indicated that the mechanism underlying the aforementioned effects was associated with the regulation of apoptosis-associated factors, including Bax, Bcl-2 and Caspase-3. Bcl-2 facilitates cell mitosis and inhibits apoptosis by regulating the outer membrane permeability of mitochondria (21,28). By contrast, Bax facilitates apoptosis by forming a heterodimer with Bcl-2 and inhibiting its function (33,41,50). Caspase-3 is an important member of the caspase family. As a conjunct activating factor in apoptosis signal transduction, it directly participates in cell regulation, signal transduction and late apoptosis (51,52). The results of the current study indicated that SUMO2 overexpression activated the apoptosis inhibitor Bcl-2 and inhibited the proapoptotic factors Bax and Caspase-3 in HG-injured H9c2 cells, thereby leading to apoptosis inhibition.

The effects of SUMO2 overexpression on the downstream effectors in the TGF-β/Smad pathway in H9c2 cells was also investigated. The TGF-β/Smad pathway is an effective signaling pathway involved in the acceleration of oxidative stress, apoptosis and inflammation, and is therefore implicated in various diseases, including cardiac fibrosis (26,53,54). Among eight Smad family members (Smad1-8), Smad2/3 and Smad4 are the critical factors in the TGF-β pathway (55). The SUMOylation of Smad3 and Smad4 have been previously reported to inhibit TGF-β/Smad transcriptional activity (56-58). The expression of Smad2/3 was also demonstrated to be regulated by HG in rat renal tubular epithelial or mesangial cells (59). Therefore, the current study focused on Smad3. The results of the current study indicated that SUMO2 overexpression significantly decreased the expression of TGF-β1 and Smad3 mRNA and protein in HG-injured H9c2 cells, indicating that SUMO2 may

function in the TGF-β/Smad pathway by inhibiting the activities of TGF-β and Smad3 in myocardial cells under HG stress conditions to inhibit cell apoptosis.

In conclusion, a HG-injured H9c2 cardiomyocyte model was established in the current study to investigate how SUMO2 overexpression alleviates cell cycle arrest and apoptosis promotion induced by HG, and the results demonstrated that this may occur via regulation of cell cycle- and apoptosis-associated factors, as well as inhibition of the TGF-β/Smad pathway. SUMO2 is downregulated by HG, therefore, it was over-expressed in the present study in order to recover it. Future studies are required to knockdown SUMO2 and to determine the effect of SUMO2 on the SUMOylation of associated factors. However, the results of the current study indicate that SUMO2 may be a potential biomarker of an important endogenous protection factor in cardiomyocytes, which may provide novel insights for the protection of cardiomyocytes and may aid in the diagnosis and prognosis of patients with DC.

Acknowledgements

Not applicable.

Funding

No funding was received.

Availability of data and materials

All data generated or analyzed during this study are included in this published article.

Authors' contributions

CZ made substantial contributions to the design of the present study and wrote the manuscript. QS made substantial contributions to the conception of the present study.

Ethics approval and consent to participate

Not applicable.

Consent for publication

Not applicable.

Competing interests

The authors declare that they have no competing interests.

References

1. Manyari DE: Prognostic implications of echocardiographically determined left ventricular mass in the Framingham Heart Study. N Engl J Med 323: 1706-1707, 1990.
2. Rohini A, Agrawal N, Koyani CN and Singh R: Molecular targets and regulators of cardiac hypertrophy. Pharmacol Res 61: 269-280, 2010.
3. Tate M, Deo M, Cao AH, Hood SG, Huynh K, Kiriazis H, Du XJ, Julius TL, Figtree GA, Dusting GJ, *et al*: Insulin replacement limits progression of diabetic cardiomyopathy in the low-dose streptozotocin-induced diabetic rat. Diab Vasc Dis Res 14: 423-433, 2017.
4. Hu X, Bai T, Xu Z, Liu Q, Zheng Y and Cai L: Pathophysiological fundamentals of diabetic cardiomyopathy. Compr Physiol 7: 693-711, 2017.
5. Mishra PK, Ying W, Nandi SS, Bandyopadhyay GK, Patel KK and Mahata SK: Diabetic cardiomyopathy: An immunometabolic perspective. Front endocrinol (Lausanne) 8: 72, 2017.
6. Prakoso D, DeBlasio MJ, Qin C, Rosli S, Kiriazis H, Qian H, Du XJ, Weeks KL, Gregorevic P, McMullen JR and Ritchie RH: Phosphoinositide 3-Kinase (p110α) gene delivery limits diabetes-induced cardiac NADPH oxidase and cardiomyopathy in a mouse model with established diastolic dysfunction. Clin Sci (Lond) 131: 1345-1360, 2017.
7. Bell DS: Diabetic cardiomyopathy. A unique entity or a complication of coronary artery disease? Diabetes Care 18: 708-714, 1995.
8. Ounzain S and Pedrazzini T: The promise of enhancer-associated long noncoding RNAs in cardiac regeneration. Trends Cardiovasc Med 25: 592-602, 2015.
9. Dhiman M and Garg NJ: NADPH oxidase inhibition ameliorates Trypanosoma cruzi-induced myocarditis during Chagas disease. J Pathol 225: 583-596, 2011.
10. Marushchak M, Lisnianska N, Krynytska capital IU and Chornomydz I: The mechanisms of apoptosis initiation in rats with chronic enterocolitis combined with streptozotocin-induced diabetes. Georgian Med News: 125-130, 2017.
11. Hong YA, Lim JH, Kim MY, Kim Y, Park HS, Kim HW, Choi BS, Chang YS, Kim HW, Kim TY, *et al*: Extracellular superoxide dismutase attenuates renal oxidative stress through the activation of AMPK in diabetic nephropathy. Antioxid Redox Signal: Nov 14, 2017 (Epub ahead of print). doi: 10.1089/ars.2017.7207.
12. Tabebi M, Khabou B, Boukadi H, Ben Hamad M, Ben Rhouma B, Tounsi S, Maalej A, Kamoun H, Keskes-Ammar L, Abid M, *et al*: Association study of apoptosis gene polymorphisms in mitochondrial diabetes: A potential role in the pathogenicity of MD. Gene 639: 18-26, 2018.
13. Bugyei-Twum A, Advani A, Advani SL, Zhang Y, Thai K, Kelly DJ and Connelly KA: High glucose induces Smad activation via the transcriptional coregulator p300 and contributes to cardiac fibrosis and hypertrophy. Cardiovasc Diabetol 13: 89, 2014.
14. Wilkinson KA and Henley JM: Mechanisms, regulation and consequences of protein SUMOylation. Biochem J 428: 133-145, 2010.
15. Princz A and Tavernarakis N: The role of SUMOylation in ageing and senescent decline. Mech Ageing Dev 162: 85-90, 2017.
16. Hay RT: SUMO: A history of modification. Mol Cell 18: 1-12, 2005.
17. Li XC, Zeng Y, Sun RR, Liu M, Chen S and Zhang PY: SUMOylation in cardiac disorders-a review. Eur Rev Med Pharmacol Sci 21: 1583-1587, 2017.
18. Guo B, Yang SH, Witty J and Sharrocks AD: Signalling pathways and the regulation of SUMO modification. Biochem Soc Trans 35: 1414-1418, 2007.
19. Geiss-Friedlander R and Melchior F: Concepts in sumoylation: A decade on. Nat Rev Mol Cell Biol 8: 947-956, 2007.
20. Rosonina E, Akhter A, Dou Y, Babu J and Sri Theivakadadcham VS: Regulation of transcription factors by sumoylation. Transcription 8: 220-231, 2017.
21. Bedford L, Lowe J, Dick LR, Mayer RJ and Brownell JE: Ubiquitin-like protein conjugation and the ubiquitin-proteasome system as drug targets. Nat Rev Drug Discov 10: 29-46, 2011.
22. Paddibhatla I, Lee MJ, Kalamarz ME, Ferrarese R and Govind S: Role for sumoylation in systemic inflammation and immune homeostasis in *Drosophila larvae*. PLoS Pathog 6: e1001234, 2010.
23. Wilson VG: Viral interplay with the host sumoylation system. Adv Exp Med Biol 963: 359-388, 2017.
24. Chang E and Abe J: Kinase-SUMO networks in diabetes-mediated cardiovascular disease. Metabolism Clin Exp 65: 623-633, 2016.
25. Shishido T, Woo CH, Ding B, McClain C, Molina CA, Yan C, Yang J and Abe J: Effects of MEK5/ERK5 association on small ubiquitin-related modification of ERK5: Implications for diabetic ventricular dysfunction after myocardial infarction. Circ Res 102: 1416-1425, 2008.
26. Zhang L, Mao Y, Pan J, Wang S, Chen L and Xiang J: Bamboo leaf extract ameliorates cardiac fibrosis possibly via alleviating inflammation, oxidative stress and apoptosis. Biomed Pharmacother 95: 808-817, 2017.
27. Xu H, Sun F, Li X and Sun L: Downregulation of miR-23a inhibits high glucose-induced EMT and renal fibrogenesis by upregulation of SnoN. Hum Cell 31: 22-32, 2018.

28. Kang JS, Saunier EF, Akhurst RJ and Derynck R: The type I TGF-beta receptor is covalently modified and regulated by sumoylation. Nat Cell Biol 10: 654-664, 2008.
29. Lin X, Liang M, Liang YY, Brunicardi FC and Feng XH: SUMO-1/Ubc9 promotes nuclear accumulation and metabolic stability of tumor suppressor Smad4. J Biol Chem 278: 31043-31048, 2003.
30. Livak KJ and Schmittgen TD: Analysis of relative gene expression data using real-time quantitative PCR and the 2(-Delta Delta C(T)) method. Methods 25: 402-408, 2001.
31. Haas AV and McDonnell ME: Pathogenesis of cardiovascular disease in diabetes. Endocrinol Metab Clin North Am 47: 51-63, 2018.
32. Singh RM, Waqar T, Howarth FC, Adeghate E, Bidasee K and Singh J: Hyperglycemia-induced cardiac contractile dysfunction in the diabetic heart. Heart Fail Rev 23: 37-54, 2018.
33. Bernt A, Rangrez AY, Eden M, Jungmann A, Katz S, Rohr C, Muller OJ, Katus HA, Sossalla ST, Williams T, *et al*: Sumoylation-independent activation of Calcineurin-NFAT-signaling via SUMO2 mediates cardiomyocyte hypertrophy. Sci Rep 6: 35758, 2016.
34. Kim EY, Zhang Y, Ye B, Segura AM, Beketaev I, Xi Y, Yu W, Chang J, Li F and Wang J: Involvement of activated SUMO-2 conjugation in cardiomyopathy. Biochim Biophys Acta 1852: 1388-1399, 2015.
35. Valle-Casuso JC, Allouch A, David A, Lenzi GM, Studdard L, Barre-Sinoussi F, Muller-Trutwin M, Kim B, Pancino G and Saez-Cirion A: p21 restricts HIV-1 in monocyte-derived dendritic cells through the reduction of dNTP biosynthesis and regulation of SAMHD1 antiviral activity. J Virol 91: e01324, 2017.
36. Brooks G, Poolman RA and Li JM: Arresting developments in the cardiac myocyte cell cycle: Role of cyclin-dependent kinase inhibitors. Cardiovasc Res 39: 301-311, 1998.
37. Hauck L, Harms C, Grothe D, An J, Gertz K, Kronenberg G, Dietz R, Endres M and von Harsdorf R: Critical role for FoxO3a-dependent regulation of p21CIP1/WAF1 in response to statin signaling in cardiac myocytes. Circ Res 100: 50-60, 2007.
38. Koga K, Kenessey A and Ojamaa K: Macrophage migration inhibitory factor antagonizes pressure overload-induced cardiac hypertrophy. Am J Physiol Heart Circ Physiol 304: H282-H293, 2013.
39. Kaplan A, Abidi E, Ghali R, Booz GW, Kobeissy F and Zouein FA: Functional, cellular and molecular remodeling of the heart under influence of oxidative cigarette tobacco smoke. Oxid Med Cell Longev 2017: 3759186, 2017.
40. Zhang D, Li Y, Heims-Waldron D, Bezzerides V, Guatimosim S, Guo Y, Gu F, Zhou P, Lin Z, Ma Q, *et al*: Mitochondrial cardiomyopathy caused by elevated reactive oxygen species and impaired cardiomyocyte proliferation. Circ Res 122: 74-87, 2018.
41. Deng H, Cheng Y, Guo Z, Zhang F, Lu X, Feng L, Wang X and Xu Z: Overexpression of cyclinA2 ameliorates hypoxia-impaired proliferation of cardiomyocytes. Exp Ther Med 8: 1513-1517, 2014.
42. Fu XJ, Li HX, Yang K, Chen D and Tang H: The important tumor suppressor role of PER1 in regulating the cyclin-CDK-CKI network in SCC15 human oral squamous cell carcinoma cells. Onco Targets Ther 9: 2237-2245, 2016.
43. Yang XH, Tang F, Shin J and Cunningham JM: Incorporating genomic, transcriptomic and clinical data: a prognostic and stem cell-like MYC and PRC imbalance in high-risk neuroblastoma. BMC Syst Biol 11 (Suppl 5): 92, 2017.
44. Liu P, Su J, Song X and Wang S: Activation of nuclear β-catenin/c-Myc axis promotes oxidative stress injury in streptozotocin-induced diabetic cardiomyopathy. Biochem Biophys Res Commun 493: 1573-1580, 2017.
45. Yoon MK, Mitrea DM, Ou L and Kriwacki RW: Cell cycle regulation by the intrinsically disordered proteins p21 and p27. Biochem Soc Trans 40: 981-988, 2012.
46. Yanagi T, Nagai K, Shimizu H and Matsuzawa SI: Melanoma antigen A12 regulates cell cycle via tumor suppressor p21 expression. Oncotarget 8: 68448-68459, 2017.
47. Zhou C, Huang J, Li Q, Zhan C, Xu X, Zhang X, Ai D, Zhu Y, Wen Z and Wang DW: CYP2J2-derived EETs attenuated ethanol-induced myocardial dysfunction through inducing autophagy and reducing apoptosis. Free Radic Biol Med 117: 168-179, 2018.
48. Chen TS, Kuo CH, Battsengel S, Pan LF, Day CH, Shen CY, Chung LC, Padma VV, Yao CK, Lin YM and Huang CY: Adipose-derived stem cells decrease cardiomyocyte damage induced by porphyromonas gingivalis endotoxin through suppressing hypertrophy, apoptosis, fibrosis and MAPK markers. Environ Toxicol 33: 508-513, 2018.
49. Wei X, Yang Y, Jiang YJ, Lei JM, Guo JW and Xiao H: Relaxin ameliorates high glucose-induced cardiomyocyte hypertrophy and apoptosis via the Notch1 pathway. Exp Ther Med 15: 691-698, 2018.
50. Yao C, Cao X, Fu Z, Tian J, Dong W, Xu J, An K, Zhai L and Yu J: *Boschniakia rossica* polysaccharide triggers laryngeal carcinoma cell apoptosis by regulating expression of Bcl-2, caspase-3 and P53. Med Sci Monit 23: 2059-2064, 2017.
51. Lv L and Liu B: Antitumor effects of bakuchiol on human gastric carcinoma cell lines are mediated through PI3K/AKT and MAPK signaling pathways. Mol Med Rep 16: 8977-8982, 2017.
52. Cui X, Jing X, Wu X, Bi X, Liu J, Long Z, Zhang X, Zhang D, Jia H, Su D and Huo K: Abnormal expression levels of BMP15/Smad1 are associated with granulosa cell apoptosis in patients with polycystic ovary syndrome. Mol Med Rep 16: 8231-8236, 2017.
53. Lustri AM, Di Matteo S, Fraveto A, Costantini D, Cantafora A, Napoletano C, Bragazzi MC, Giuliante F, De Rose AM, Berloco PB, *et al*: TGF-β signaling is an effective target to impair survival and induce apoptosis of human cholangiocarcinoma cells: A study on human primary cell cultures. PLoS One 12: e0183932, 2017.
54. Qiu M, Chen Y, Chen L, Zeng J and Liu J: Transforming growth factor β1 and Fas ligand synergistically enhance immune tolerance in dendritic cells in liver transplantation. J Surg Res 218: 180-193, 2017.
55. Chen K, Cheng L, Qian W, Jiang Z, Sun L, Zhao Y, Zhou Y, Zhao L, Wang P, Duan W, *et al*: Itraconazole inhibits invasion and migration of pancreatic cancer cells by suppressing TGF-beta/SMAD2/3 signaling. Oncol Rep 39: 1573-1582, 2018.
56. Imoto S, Sugiyama K, Muromoto R, Sato N, Yamamoto T and Matsuda T: Regulation of transforming growth factor-beta signaling by protein inhibitor of activated STAT, PIASy through Smad3. J Biol Chem 278: 34253-34258, 2003.
57. Imoto S, Ohbayashi N, Ikeda O, Kamitani S, Muromoto R, Sekine Y and Matsuda T: Sumoylation of Smad3 stimulates its nuclear export during PIASy-mediated suppression of TGF-β signaling. Biochem Biophys Res Commun 370: 359-365, 2008.
58. Long J, Wang G, He D and Liu F: Repression of Smad4 transcriptional activity by SUMO modification. Biochem J 379: 23-29, 2004.
59. Tang WB, Ling GH, Sun L, Zhang K, Zhu X, Zhou X and Liu FY: Smad anchor for receptor activation regulates high glucose-induced EMT via modulation of Smad2 and Smad3 activities in renal tubular epithelial cells. Nephron 130: 213-220, 2015.